WATER RESOURCES RESEARCH, VOL. 36, NO. 8, PAGES 2121–2132, AUGUST, 2000

Inferring the relation between seismic slowness and hydraulic conductivity in heterogeneous aquifers

David W. Hyndman
Department of Geological Sciences, Michigan State University, East Lansing

Jerry M. Harris
Department of Geophysics, Stanford University, Stanford, California

Steven M. Gorelick
Department of Geological and Environmental Sciences, Stanford University, Stanford, California

Abstract. Cross-well seismic tomography can be used to develop high-resolution seismic slowness (1/velocity) estimates along planes through aquifers. Unfortunately, the relation between seismic slowness and hydraulic conductivity is poorly understood, resulting in poor characterization of hydraulic properties from seismic data. This relation is generally developed from laboratory measurements, but slowness values measured with very high frequencies in the lab are often poorly correlated with lower frequency cross-well and surface seismic slowness values. To address this problem, we developed an approach to infer the relation between slowness and hydraulic conductivity using field scale geophysical and hydrogeologic measurements. We first develop an a priori relation between the conductivity measurements and the cross-well slowness estimates. Multiple three-dimensional slowness realizations, conditioned on the cross-well estimates, are then generated and remapped into log conductivity fields using the a priori slowness to log conductivity relation. We simulate groundwater flow and tracer transport through these conductivity fields and calculate the residuals between measured and simulated concentration arrival time quantiles and drawdown. The slope and intercept of the relation between slowness and log hydraulic conductivity and the dispersivity are then estimated for each slowness realization to minimize the sum of these squared residuals. We demonstrate this approach for the Kesterson aquifer, California, where seismic tomography provided valuable information about aquifer properties. The groundwater flow and tracer transport simulations, through the estimated conductivity fields, yield reasonable fits to the observed tracer concentration histories for two multiple-well tracer tests (one of which was not used in the inversion) and to the measured drawdown. This approach provides estimates of seismic slowness and hydraulic conductivity, and information about the relation between slowness and log conductivity for a field site.

1. Introduction

Inferring heterogeneous aquifer properties has become a critical research topic in hydrogeology. Groundwater flows preferentially along high hydraulic conductivity paths within the three-dimensional structure of an aquifer. Accurate estimation of heterogeneous flow properties is critical to predict solute transport along such paths.

Estimating values of subsurface hydraulic properties is difficult because the environment is largely inaccessible and common measurements used to deduce these properties are sparse. Geophysical measurements could provide the needed high-resolution estimates of aquifer properties, but the relations between the estimated geophysical properties and the desired hydraulic properties are unknown at the field scale. An improved understanding of these relations would allow more quantitative use of geophysical measurements to estimate hydraulic properties.

Many researchers have tried to explain the relations between geophysical and hydraulic properties at the lab scale. In this paper we focus on relations between seismic slowness (1/velocity) and hydraulic conductivity at the field scale where we have high-resolution cross-well slowness estimates, called tomograms. Relations may also exist between hydraulic conductivity and both the seismic attenuation coefficient [*Prasad and Meissner*, 1992] and the dielectric constant (estimated using ground-penetrating radar measurements) [*Beres and Haeni*, 1991; *Knoll et al*., 1991]. The velocity of seismic energy is a function of the elastic properties (density, bulk modulus, and shear modulus) of the media [*Telford et al*., 1990], which depend on both lithologic and fluid properties. Several empirical averaging equations and transforms were developed between seismic velocity and porosity [*Raymer et al*., 1980; *Wyllie et al*., 1956]. *Han et al*. [1986] showed that adding clay content as an additional parameter could reduce much of the scatter in these empirical relations. *Marion et al*. [1992] developed a conceptual model to describe the relationship between seismic veloc-

Paper number 2000WR900112.
0043-1397/00/2000WR900112$09.00

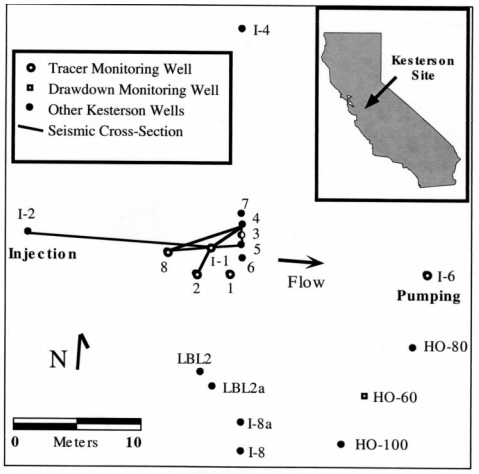

Figure 1. Site map for the Kesterson aquifer located in the California San Joaquin Valley.

ity and porosity of sand-clay mixtures. *Rubin et al*. [1992], *Copty et al*. [1993], and *Copty and Rubin* [1995] used Marion's relation between seismic velocity and permeability in stochastic inversions for permeability fields. *McKenna and Poeter* [1995] classified the hydrofacies of an aquifer using seismic velocities, hydraulic test data, and geologic information.

Although lab-based empirical relations may provide some insight into the field scale relations, they often have limited predictive power. Several complicating factors, such as seismic velocity dispersion and sample alteration, limit the use of lab-based relations for field prediction. Velocity dispersion is a frequency-dependent mechanism [*Bourbie et al*., 1987], thus ultrasonic velocities measured in the laboratory will probably be different from velocities measured with lower frequencies in the field. In addition, cores taken from the field are always disturbed, and field conditions are not reproduced in the laboratory, resulting in different properties at lab and field scales. At a slightly larger scale, relationships could be derived on the basis of well logs, but a similar range of uncertainty exists in these estimated seismic velocity values because well bores are disturbed during drilling.

Instead of estimating the relation at the lab scale for prediction at the field scale, we combine field scale seismic and hydrologic data to estimate the relation for a particular site. This estimated field relation could then be used for nearby sites with a similar depositional environment, assuming the relation is stationary across the region. This approach does not assume scale independence, which is required to use lab-based relations at the field scale. The nature of the estimated relation will depend on the types of available field data.

In this paper we demonstrate a new approach to estimating aquifer parameters which infers a relation between seismic slowness and log hydraulic conductivity. In the presented field application, we estimate a linear relation between these properties because the data do not appear to support a more complex relation. For a linear relation, this approach involves only three parameters: the slope and intercept of the relation and the dispersivity used in the tracer simulations. We combine cross-well seismic tomography with core measurements, pump tests, and a multiple-well tracer test to infer this relation and the dispersivity for the Kesterson aquifer. The slope and intercept of this relation, and the dispersivity, are adjusted to best match simulated and observed tracer and drawdown data. The dispersivity estimate is only sensitive to the tracer simulations in this algorithm. A second forced gradient tracer test in a direction perpendicular to the first is used to check the estimated conductivity and dispersivity estimates.

The philosophy underlying this inversion is that a relation between slowness and log conductivity may exist, but this relation is most useful if it has been developed at the field scale for which it will be used. Estimating such a relation at the field scale provides a valuable tool for in situ aquifer property estimation. When such a relation is estimated for a particular depositional environment, it could be used to convert nearby seismic tomograms into initial estimates of hydraulic properties assuming stationarity of the approach. This would allow for more accurate solute transport predictions in regions with little available hydraulic data by incorporating extensive seismic data.

2. Overview of the Kesterson Site

The Kesterson aquifer, which is located in the California San Joaquin Valley (Figure 1), has been characterized in detail during the last decade because of selenium contamination of both surface water and groundwater. Agricultural return waters containing high concentrations of selenium and other contaminants were discharged to the Kesterson Reservoir in the early 1980s. Approximately 50% of this return water infiltrated, creating a large groundwater contaminant plume. The predominant lithology at the site is clean sand that was deposited by the meandering San Joaquin River. Several data sets were collected to characterize the shallow Kesterson aquifer, including seismic travel times between six well pairs and six tracer concentration histories during two forced gradient tests.

Benson [1988] conducted two tracer tests using an injection/withdrawal well pair and multiple observation wells at different depths. The first tracer test was conducted in 1986 by pumping 4.7 L/s from well LBL-I6 and injecting this water back into well LBL-I2, which is ~30 m to the west. The injection/withdrawal well pair was pumped for 24 hours prior to the tracer test in order to approach a steady state flow field. A concentrated fluorescein solution was then added to the injection stream for 3180 s (0.883 hours) to achieve a total injection concentration of ~320 ppm. Concentrations were then monitored at six wells throughout the 10 day tracer test (Wells 1, 2, 3, 8, I1, and I6; see Figure 1 for locations). In 1988, a second tracer test was performed perpendicular to the 1986 test with water pumped from well LBL-I8a and injected back into well LBL-I4 with amended fluorescein tracer. Fluorescein is a weekly sorbing tracer as determined by *Smart and Laidlaw* [1977] using batch experiments with different sediments. Thus for this study we assume that fluorescein is a conservative tracer.

Seismic travel times between multiple sources and multiple receivers, from Ernie Majer at Lawrence Berkeley Laboratory, provided the second main data source for this work. These data are derived by calculating the times for each pulse of seismic energy (sound waves) to propagate from a source well to multiple receiver locations in nearby wells. For this test, the seismic source was a piezoelectric bender bar with a frequency range of 6–10 kH, and the receivers were hydrophones. The vertical spacing of both the receivers and the sources was 0.3 m in this case, and between 13 and 29 source receiver locations were available for each well pair. Additional details of the geophysical data collection and analysis are available in the works of *Hyndman and Gorelick* [1996] and *Hyndman and Harris* [1996].

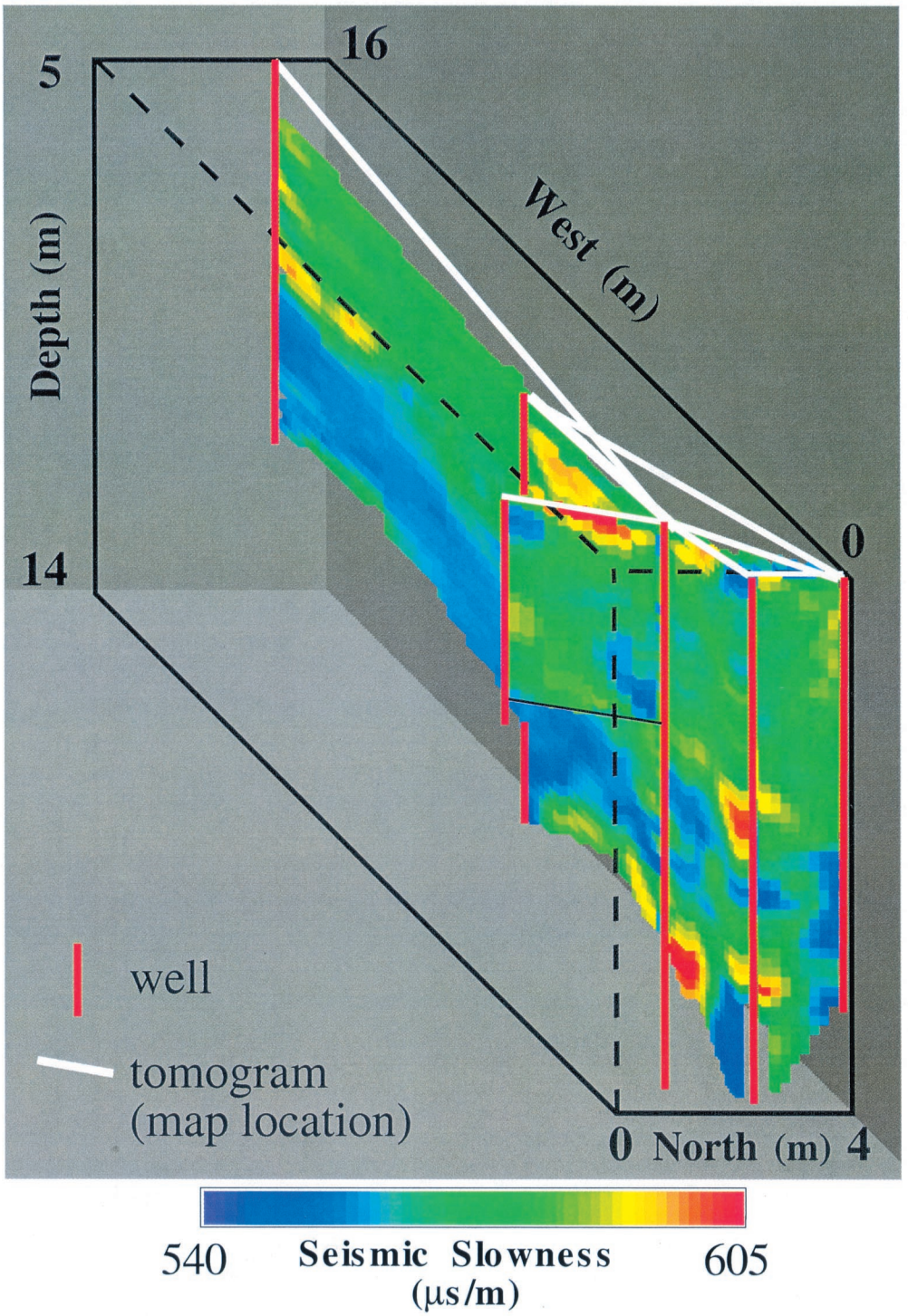

Plate 1. Three-dimensional layout of seismic slowness estimates at the Kesterson site from *Hyndman and Harris* [1996]. Wells ST5 and ST4 are on the close side of the image and Well I2 is at the top.

Our earlier work on the Kesterson site indicated that a relation between slowness and conductivity might exist for this site. *Hyndman and Harris* [1996] coinverted the six cross sections of seismic travel times for three seismic slowness populations that probably represent different lithologies. They then generated multiple three-dimensional conditional realizations of seismic slowness and estimated the zonation of lithologies, hydraulic conductivity values for each zone, and a regional value of dispersivity for five realizations based on the tracer data. *Hyndman and Gorelick* [1996] used the Split Inversion Method (SIM) to split each slowness realization into zones and estimate the conductivity values for these zones to minimize the squared residuals between simulated and observed tracer concentration histories. The SIM is designed to estimate the lithologic structure of an aquifer even in cases of a nonlinear and nonunique relation between slowness and log hydraulic conductivity [*Hyndman et al.*, 1994], yet at the Kesterson site the results indicate a linear trend between the tomographic

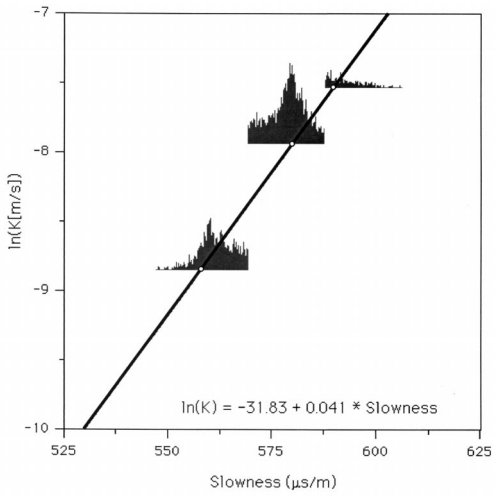

Figure 2. Linear fit between slowness and natural log conductivity estimates from the split inversion method (SIM) [*Hyndman and Gorelick*, 1996]. The 41,440 values represent slowness estimates from a 3-D realization versus the hydraulic conductivity values assigned by SIM for the corresponding points. The slowness values prior to the split are illustrated by the histograms.

slowness estimates and the zonal log hydraulic conductivity estimates (Figure 2). The SIM matched the main features of the tracer concentration histories using reasonable estimates of the hydraulic parameters and geologically reasonable lithologic zonations for the site [*Hyndman and Gorelick*, 1996]. However, this involved a great deal of computation to resolve six parameters (two slowness values that split the realizations into three zones, an effective hydraulic conductivity value for each of the three zones, and a regional dispersivity value) for each slowness realization.

Here we build on this earlier work and develop a new approach to estimate a hydraulic conductivity field from seismic, hydraulic, and tracer data by inferring a simple relation between slowness and log hydraulic conductivity. This new approach provides several advances, including (1) the ability to represent smaller-scale variations in hydraulic conductivity than possible with a zonal estimation method, (2) reduced computational time because few parameters are needed to represent the relation, and the parameters can be defined to be sensitive to different data sets (i.e., tracer concentrations and drawdown), and (3) information about potential relations between geophysical and hydrogeologic parameters using field scale data sets.

3. Inversion Method

The main steps of our new approach are as follows:

1. Invert seismic travel times measured between well pairs for seismic slowness fields (tomograms) using the multiple-population inversion approach of *Hyndman and Harris* [1996], and update these estimates using a traditional tomographic inversion.

2. Generate equally likely conditional slowness simulations using sequential Gaussian simulation as described by *Hyndman and Gorelick* [1996].

3. Estimate an a priori relation between seismic slowness and log hydraulic conductivity using available field data.

4. Use the a priori relation to map slowness realizations into log hydraulic conductivity fields for groundwater flow and solute transport simulations, and calculate the residuals between measured and simulated drawdown at well HO60 (see Figure 1 for location) and concentration arrival histories.

5. Systematically perturb the estimated relation between slowness and log conductivity to minimize the sum of squares of these residuals.

We describe these steps in more detail below.

We began with the multiple population inversion approach of *Hyndman and Harris* [1996] to invert seismic travel times between six well pairs for seismic slowness tomograms (estimated vertical cross sections). This method iteratively coinverts the travel times from all six well pairs for the best spatial distribution of three slowness populations. In other words, the geometry of these three slowness zones and the slowness value for each zone were iteratively adjusted to minimize the residuals between measured and simulated seismic travel times. This approach provided high-resolution estimates (0.4 m vertical and 1.5 m horizontal) of the seismic slowness structure of the Kesterson aquifer along these cross sections. These tomograms were then updated using a traditional tomographic inversion to provide more continuous slowness estimates (Plate 1).

Equally likely three-dimensional conditional realizations of slowness were then generated using a geostatistical method called sequential Gaussian simulation [*Deutsch and Journel*, 1992]. This approach honors the values at all seismic tomogram locations, as well as the sample probability distribution and variograms of the tomographic slowness estimates. We calculated sample variograms for the slowness tomograms in Plate 1 and fit exponential variograms (horizontal correlation length is equal to 5–9 m, vertical correlation length is equal to 0.9 m, population variance is equal to 104) to these sample variograms to explore the probable range of correlation lengths [*Hyndman and Gorelick*, 1996]. Insufficient seismic data were available to detect any horizontal anisotropy at the site; so we used isotropic variograms in the horizontal direction.

We then developed an a priori relation between seismic and hydraulic parameters, which we later updated using a simulation-regression approach to obtain the best match to the available field data. One method to infer the a priori relation between slowness and conductivity is to analyze the slowness and conductivity of core samples in the lab. However, *Copty* [1994] found very little correlation between lab-measured ultrasonic velocity (or slowness) and lab-measured log hydraulic conductivity values (Table 1, data collected by Jill Geller at Lawrence Berkeley Laboratory) for nine sections taken from a single continuous core at the Kesterson site (Figure 3, correlation coefficient is equal to 0.16).

Although the laboratory data showed very little correlation, the Kesterson field data indicate that a relationship may exist. Using the field data, we developed an a priori relation between the estimated zonal slowness tomograms from *Hyndman and Harris* [1996] and the hydraulic conductivity estimates from both core samples and pump tests in the region of these seismic tomograms. The primary lithology at the site is clean unconsolidated sand with regions of higher clay content. These data are summarized in Figure 4, which illustrates the best fit linear relation between log hydraulic conductivity from both pump tests and core data and the seismic slowness estimates from tomography. Although the confidence in this fit is low (correlation coefficient is equal to 0.74), the slowness values estimated at the field scale are better correlated to hydraulic

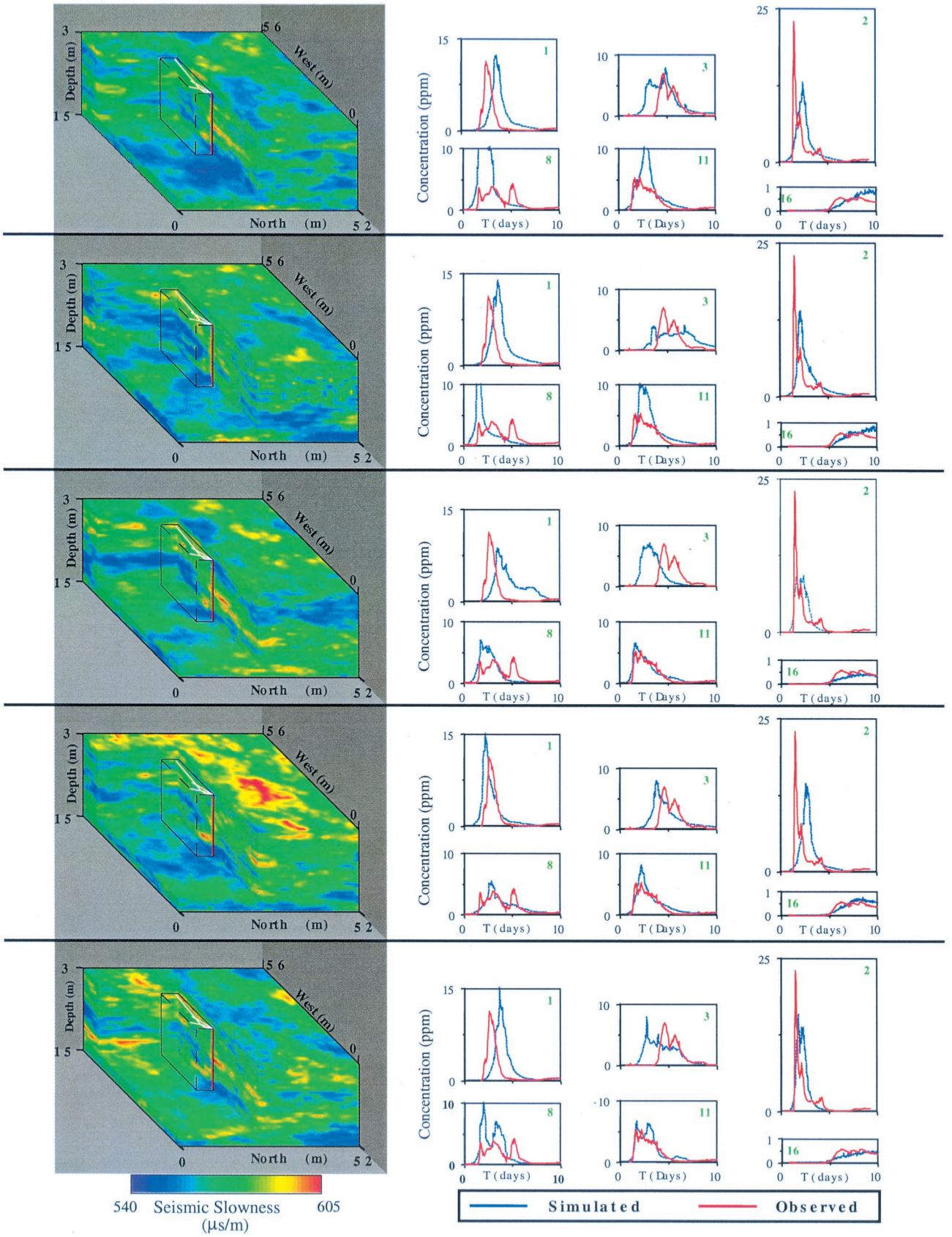

Plate 2. Slowness realizations with corresponding simulated and observed concentration histories for the six tracer monitoring wells noted in Figure 1, with well numbers noted within each concentration history box.

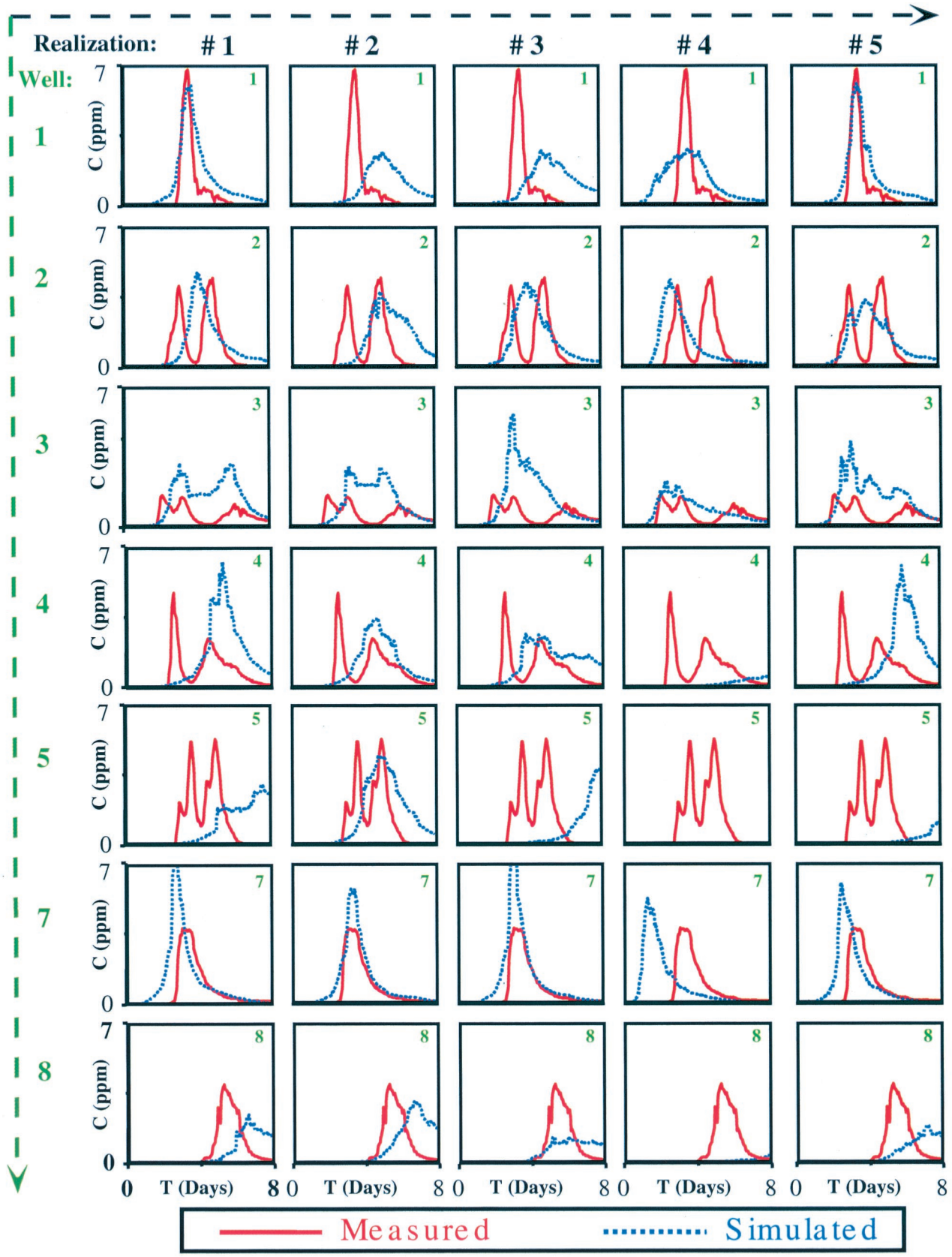

Plate 3. Simulated and observed tracer concentration histories for the 1988 fluorescein tracer test from Wells I4 to I8a. The well numbers are located in the top right corner of each graph (see Figure 1 for locations).

conductivity estimates than the lab-measured ultrasonic slowness values.

The pump test conductivity estimates from *Benson et al.* [1991] are plotted in Figure 4 with respect to the average of the zonal slowness estimates adjacent to the well screen interval. The slowness estimates were averaged because the pump test measures an average conductivity across a region with higher-resolution tomography estimates. A nonlinear relation could also be fit between the slowness and the log conductivity estimates, but a log-linear relation appears to be adequate given the limited information available. The core samples were taken ~0.9 m from Well 5 along the cross section toward Well I1 (Figure 1). At this site, log conductivities from the cores are plotted versus the tomographic slowness estimates from *Hyndman and Harris* [1996], since these provide the highest-resolution seismic estimates available in the region of the collected core. The best linear fit between the tomographic slowness values (μs/m) and the log conductivities (m/s) from both core and pump tests (Figure 4) is given by (1) below.

The relation in (1) is used to map each slowness realization into an initial estimate of the log conductivity field.

$$\ln (K) = a + bS \tag{1}$$

where

a intercept = 31.55
b slope = 0.0411
K hydraulic conductivity, {m/s}
S seismic slowness, {μs/m}.

Each log conductivity field is then used as input to a three-dimensional groundwater flow and solute transport model for the region. MODFLOW [*McDonald and Harbaugh*, 1988] was used for the groundwater flow simulations and MT3D [*Zheng*, 1992] was used for the tracer transport simulations because of the dominance of advection at the site.

For each realization the dispersivity and the slope and intercept of the slowness to log conductivity relation were adjusted to best match the tracer and drawdown measurements. The initial value of dispersivity was chosen based on earlier work at the Kesterson site, although the inversion routine was not sensitive to this initial estimate. Each time the slope or intercept is adjusted, the slowness realization is mapped into a log hydraulic conductivity field (Plate 2), which is used in groundwater flow and tracer transport simulations. The simulated drawdown and concentration histories are compared to available measurements (Plate 2) for each adjustment. The slope and intercept are adjusted to minimize the weighted sum of squared residuals between measured and simulated drawdown at well HO60 and concentration arrival time quantiles at six observation wells. The nine quantiles for each observation well represent the times at which 10–90% of the tracer passes the well. The slope and intercept of the slowness to log conductivity relation and the dispersivity are adjusted to minimize the objective value (2).

$$\text{Minimize} \left(\sum_{i=1}^{9} (\tau^{w}_{i,\text{meas}} - \tau^{w}_{i,\text{sim}})^2 + \beta(\Delta h^{w}_{i,\text{meas}} - \Delta h^{w}_{i,\text{sim}})^2 \right) \qquad w = 1, 2, 3, I2, I6 \tag{2}$$

Table 1. Slowness and Conductivity Measurements in a Core Near Well ST5

Depth, m	Tomogram* Slowness, μs/m	ln K, m/s	Lab Slowness, μs/m	Effective Pressure,† KPa	
				Axial	Lateral
3.78	···	−9.1475	561.80	68.95	27.58
3.84	···	−8.9688	549.45	68.95	27.58
5.15	578.92	−8.0972	571.43	82.74	34.48
5.18	558.91	−7.7161	568.18	75.85	27.58
5.28	558.91	−8.6195	529.10	55.16	55.16
6.47	558.91	−9.0844	540.54	62.06	27.58
6.54	595.65	−6.9822	549.45	62.06	27.58
6.60	578.92	−7.8492	571.43	68.95	27.58
6.66	578.92	−7.4831	537.63	75.85	27.58

Core is ~0.9 m from Well ST5 in the plane of the seismic tomogram toward Well I1 (laboratory data collected by J. Geller, LBL; N. Copty, personal correspondence, 1994).

*The estimated tomographic slowness values were developed using the multiple population inversion approach of *Hyndman and Harris* [1996].

†Data presented for the lowest available effective pressures, although each sample was analyzed for two to three effective pressures as presented by *Copty* [1994].

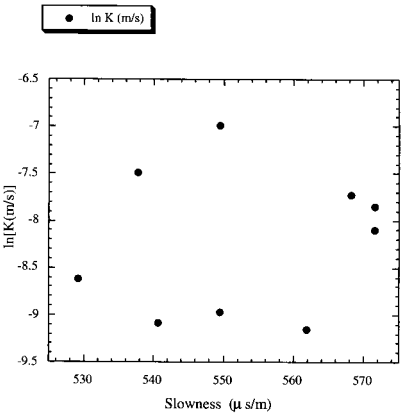

Figure 3. Scatterplot of lab-measured seismic slowness versus natural log hydraulic conductivity values from a core collected at the Kesterson field site. There is no meaningful correlation between these data sets (correlation coefficient = 0.16).

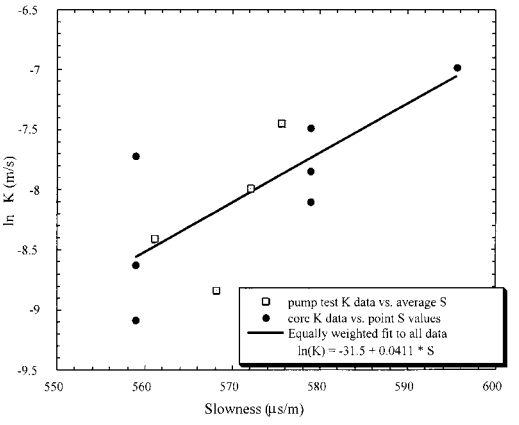

Figure 4. A priori relation between field-based tomographic seismic slowness estimates and natural log hydraulic conductivity estimates from seven core segments and four pump tests (correlation coefficient = 0.75). Tomographic slowness values are averaged across the screened interval for comparison to pump test data. Values for this plot are also shown in Table 1.

where

$\tau^w_{i,\mathrm{meas}}$ ith measured concentration arrival time quantile for well w (days);
$\tau^w_{i,\mathrm{sim}}$ ith simulated concentration arrival time quantile for well w (days);
i arrival time quantile index (−);
w well identification index (see Figure 1 for locations) (−);
β weight to provide sensitivity to both the tracer and the drawdown data ((days/m)^2);
Δh_{meas} measured drawdown at well HO60 (see Figure 1 for location) (m);
Δh_{sim} simulated drawdown at well HO60 (m).

The weighting factor (β) can be adjusted to normalize the contribution of different data sets. The weighting factor is most important when the two data sets have different minima, and thus the assigned weight locates the parameter estimates somewhere in between the individual minima. In all cases there is an implicit weight because of the units specified for the two data sets. For example, if the drawdown were measured in centimeters, the squared drawdown residuals would have an implicit weight 10,000 times larger than if drawdown were measured in meters, given no change in the units of concentration arrival time quantiles. In this case, a weight of 10,764 provided sufficient sensitivity to both the hydraulic and the tracer data. For this Kesterson inversion the weighting factor had little effect on the estimated parameters, although the convergence rate differed. This is because the simulated drawdown is primarily sensitive to the intercept of the slowness to log conductivity relation, while the simulated tracer concentration arrival time quantiles are primarily sensitive to the slope and the dispersivity.

Concentration arrival time quantiles were used in the objective function because of the complex nature of the concentration histories. Originally, we used the squared difference between measured and simulated concentrations through time at all locations. However, this objective had poor convergence when the parameters were far from their optimal values and the simulated and measured concentration histories did not significantly overlap. In this case, the squared concentration residuals are not very sensitive to small adjustments in the conductivity field. An objective based on concentration quantiles is more robust because it avoids penalizing peaks with correct magnitudes and incorrect timing, which occurs when the objective is based on the squared concentration residuals.

To remove the dependence between slope and intercept, we removed the median of the estimated slowness values from the intercept (Table 2).

$$\ln(K) = (a + bS_{\mathrm{median}}) + b(S - S_{\mathrm{median}}), \quad (3)$$

where $a = -31.55$ and $b = 0.0411$,

$$\ln(K) = c + b(S - S_{\mathrm{median}}), \quad (4)$$

where the modified intercept $c = (a + bS_{\mathrm{median}})$. This procedure reduces the dependence between the slope and the intercept and thus provides a better parameter set for this inversion. Adjustments in the slope of (3) do not require a corresponding change in modified intercept (c) to maintain a reasonable relation between slowness and log conductivity. For a particular slowness realization the median slowness is used to calculate the modified intercept of the a priori relation (1).

Table 2. Minimum Squared Residuals for Parameters From Table 3

Realization	Median Slowness, μs/m	Drawdown Residual, m^2	$\Sigma(\tau_{\mathrm{mes}} - \tau_{\mathrm{sim}})^2$ (day^2)	Total Weighted Residual (day^2)
1	571.73	2.94×10^{-5}	40.40	40.72
2	570.38	2.32×10^{-6}	51.95	51.98
3	575.88	8.18×10^{-6}	95.74	95.83
4	573.42	1.86×10^{-4}	15.45	17.49
5	574.55	6.97×10^{-5}	36.10	36.86

Using our developed inversion method, we infer the relation between conductivity and slowness from field data and generate probable hydraulic conductivity fields for the Kesterson aquifer.

4. Kesterson Results

The approach detailed above provided reasonable fits to the tracer and drawdown data using only three parameters, the slope and intercept of the seismic slowness to natural log conductivity relation (4) and a single value of longitudinal dispersivity for the region (transverse dispersivity assumed to be 0.2 × longitudinal dispersivity). Five slowness realizations were generated (Plate 2) using sequential Gaussian simulation, each with the same statistical parameters ($\lambda_h = 9$ m, $\lambda_v = 0.9$ m, $\sigma^2 = 104$). Each realization was then mapped into a natural log conductivity field using the a priori relation in (3), providing an initial conductivity field for groundwater flow and tracer transport simulations. The slope and intercept of this relation and the dispersivity were then adjusted to obtain the best fit between measured and simulated tracer arrival time quantiles and drawdown.

The simulated concentration histories are illustrated in Plate 2 for the optimal parameters listed in Table 3, along with the observed concentration histories for the six sampled observation points. The simulated concentration histories provide a reasonable match to the observed data although, as expected, the fits differ from one realization to the next (Plate 2) due to differences in the estimated hydraulic conductivity fields. The main features of the concentration arrival histories are reproduced in all but a few cases. The drawdown and concentration quantile residuals are listed in Table 2 for the five randomly chosen realizations. The best fit to the objective function (2) was for realization 4, which also provided the best visual fit of the measured and simulated concentration histories.

Table 3. Optimal Parameter Estimates for the Tracer and Drawdown Data

Realization*	Slope†	Intercept†	Modified intercept‡	Dispersivity, m
1	0.032	−26.576	−8.375	0.076
2	0.036	−28.838	−8.145	0.091
3	0.037	−29.595	−8.175	0.091
4	0.058	−41.586	−8.195	0.096
5	0.040	−30.916	−8.145	0.061

*Slowness realizations in Plate 2.
†Slope and intercept of slowness (μs/m) to natural log conductivity (m/s) relation ($\ln(K) = a + b^*S$).
‡Modified intercept = $(a + bS_{\mathrm{median}})$ from equation (4).

We found that the estimated parameters converged from different starting points to approximately the same objective values. For example, the slope converged to a value of 0.032 for realization 1 from a starting value of 0.061 as well as from the a priori starting value of 0.041. The estimated slope and intercept are similar to the a priori estimates, indicating that in some cases, pump test and core data may be used in conjunction with seismic tomography to provide a reasonable a priori relation between slowness and log conductivity. The a priori estimates for the Kesterson example, however, were mainly used to justify the linear shape of the slowness to log conductivity relation.

Multiple equally likely slowness realizations were used to explore a portion of the likely relations between slowness and log hydraulic conductivity and gain some insight into the uncertainty of the estimated relation. The estimated slope and intercept of (4) and dispersivity for each realization are listed in Table 3. The differences between realizations allow us to approximate parameter uncertainty. The mean and standard deviation of these parameters are slope (mean = 0.041, σ = 0.010), intercept with median slowness removed (mean = −8.21, σ = 0.096), and dispersivity (mean = 0.083 m, σ = 0.014 m). The transverse dispersivity was fixed at 0.2 times the longitudinal value for all simulations. To fully characterize the uncertainty in these parameters would involve many more realizations and an analysis of the potential measurement and modeling errors.

At the Kesterson site, there was no meaningful correlation between the lab-measured hydraulic conductivity and ultrasonic slowness measurements (Figure 3), yet the lab-measured conductivity values appear to be correlated to our tomographic slowness estimates (Figure 4). The estimated mean slope and modified intercept (median slowness removed) of the relation between slowness (μs/m) and natural log conductivity (m/s) of 0.041 and −8.21 compare favorably to the a priori estimates of 0.041 and −7.95 (from Plate 1, using the median tomogram slowness of 574.2 μs/m). This indicates that the a priori relation between field scale slowness values and conductivity values from cores and pump tests was reasonable. The linear fit of estimates from *Hyndman and Gorelick* [1996] also provided similar values of 0.041 and −8.33 (from Figure 2, using the median slowness of 574.2 μs/m). The estimated dispersivity 0.083 m is larger than the 0.03 m value estimated by *Benson* [1988], who used a one-dimensional analysis of the 1986 tracer test used in this study.

4.1. Independent Tracer Test Comparison

To check our parameter estimates, we simulated solute transport for an independent tracer test that was conducted perpendicular to the 1986 tracer test. *Benson* [1988] conducted this tracer test in 1988 by pumping 5.1 L/s from well LBL-I8a and injecting this water back into well LBL-I4. The injection and withdrawal wells were pumped for 24 hours prior to the tracer test to develop a steady state flow field. A concentrated fluorescein solution was then pumped into the injection stream for 64 min to achieve a total injection concentration of ~140 ppm. Concentrations were monitored at seven wells located near the center of the pumping/withdrawal well pair (Wells 1, 2, 3, 4, 5, 7, and 8; see Figure 1 for locations). The coordinates of these wells and the depth of the 1.5 m screened intervals are listed in Table 4.

Plate 3 illustrates the simulated and observed concentration histories for the five slowness realizations in Plate 2 using the estimated parameters from Table 3. The central tendency of 26 of the 35 illustrated concentration histories for the 1988 tracer test are reproduced without adjusting the parameters estimated using the 1986 tracer data. The reproduction of the primary features of the concentration histories for this independent data set indicates that for this site, our approach provides useful aquifer property estimates.

Most of the seismic data were collected in the primary direction of groundwater flow for the 1986 tracer test. The 1988 tracer test was performed perpendicular to the 1986 test, resulting in less constrained conductivity values along the primary flow paths for the 1988 test (see site map in Figure 1). The conductivity changes most from one realization to the next near the injection and withdrawal wells I4 and I8a for the 1988 test. As a result, there are significant differences between the simulated concentration histories for different realizations (Plate 3). Realization 2 provides the best overall match to the 1988 data, while realization 4 provides the worst match. This indicates the importance of data acquisition across the entire region of interest, because the simulated tracer concentrations are much closer to the measured values for the 1986 tracer test along a path where densely collected seismic data were available.

Table 4. Hydraulic Conductivity Values From Pump Tests at the Kesterson Site [after *Benson*, 1988]

Well	North, m	West, m	Top of Screen, m	Bottom of Screen, m	ln K, m/s
I1	−1.50	2.34	6.10	12.19	−7.98
I2	−0.48	16.12	6.10	12.19	−8.49
I4	14.21	0.00	6.10	12.19	−7.77
I6	−3.40	−13.87	6.10	12.19	−8.89
I8	−16.34	0.06	6.10	12.19	−8.13
I8a	−14.21	0.00	6.10	12.19	···
LBL2	−10.59	3.11	6.50	8.00	−8.76
LBL2A	−11.67	2.10	10.67	12.19	−7.34
HO100	−15.76	−7.54	24.38	30.48	−7.98
HO80	−8.74	−12.80	18.29	24.39	−8.70
HO60	−12.26	−9.44	12.19	18.30	−8.89
ST1	−3.38	0.96	6.10	7.60	−7.42
ST2	−3.43	3.37	7.60	9.10	−7.44
ST3	−0.65	−0.05	9.10	10.60	−8.76
ST4	0.09	0.00	10.60	12.19	−8.35
ST5	−1.36	−0.03	12.19	13.72	···
ST6	−2.17	0.00	4.57	6.1	···
ST7	0.91	0.10	7.62	9.14	···
ST8	−1.83	5.63	10.67	12.19	···

4.2. Incorporation of Hydraulic Conductivity Measurements

4.2.1. Sequential Gaussian simulation of conductivity data. Geostatistical methods can also be used to develop hydraulic conductivity estimates based on the available hydraulic conductivity measurements if information exists about the spatial correlation of this property in space. In this case we used a sequential Gaussian simulation algorithm [*Deutsch and Journel*, 1992] to generate log hydraulic conductivity realizations conditional to the conductivity measurements from steady state pumping tests from the Kesterson site using the correlation lengths from the seismic tomography. If the seismic tomography estimates were not available for this site, the correlation lengths would have to be estimated using other information such as continuous cores sampled for hydraulic conductivity. The measured conductivity values are listed in Table 4 with the corresponding measurement locations. We assigned

the measured conductivity values to a single cell (0.4 m vertical and 1.5 m on a side) at the central depth along the screened interval and generated all other estimates using sequential Gaussian simulation. The realization illustrated in Plate 4a was generated using the same correlation lengths as used for the generation of slowness realizations (λ_h = 9 m, λ_v = 0.9 m). The mean and variance for this realization were taken from the natural log conductivity measurements (σ^2 = 0.32, mean = −8.208).

These conductivity measurements, which are mostly at the tracer sampling wells, provide a reasonable representation of subsurface heterogeneities in the region of the 1986 and 1988 tracer tests. A randomly chosen realization is illustrated in Plate 4a along with the simulated and observed tracer concentration histories. These simulated concentration histories show similar features to those in Plate 2, which indicates that the two different conditioning data sets (seismic slowness and hydraulic conductivity) provide complimentary information.

The most notable difference is that the slowness realizations are more heterogeneous than the conductivity realization in Plate 4a, which has a more layered appearance. This higher degree of variability in the seismic estimates is expected since the seismic information provides higher-resolution information about interwell heterogeneities than the more sparsely sampled conductivity measurements. The match between measured and simulated tracer concentration histories at the withdrawal well (I6) and well 1 were better using the rescaled seismic slowness fields than simulated using conductivity data alone. This indicates that the seismic information can provide valuable information about the heterogeneous hydraulic conductivity field. The match to the concentration histories is similar at the other wells for both methods.

4.2.2. Sequential Gaussian cosimulation of conductivity and slowness data. Since a linear relation between seismic slowness and log hydraulic conductivity appears to be reasonable for the Kesterson site, the seismic data can be used as soft data in a sequential Gaussian cosimulation algorithm [*Deutsch and Journel*, 1992]. We used this algorithm to generate conductivity realizations based on a correlation coefficient of +0.74, as calculated from Figure 4, to incorporate the soft seismic estimates with the hard conductivity data. Plate 4b illustrates a randomly chosen realization with the same random path that was used to generate Plate 4a. For this realization we used the entire fourth slowness realization as soft data and conditioned to the hard conductivity data in Table 4. We also generated realizations that only used tomographic seismic estimates as soft data and found that these conductivity realizations resulted in poor matches to the measured concentration histories.

In this case, the slowness estimates improved the concentration histories at all wells except at Well 8, relative to the simulations through the estimate from conductivity data alone (Plate 4a). However, relative to the estimates made using our approach of inferring the relation between slowness and log conductivity (Plate 2), these sequential Gaussian cosimulation estimates provide a poorer match to the tracer data. The least squared tracer quantile residual was 47.2 day^2 for this cosimulation case, while it was 15.45 day^2 for the case where we estimated the relation between slowness and log conductivity. This is mostly because the fits for the estimated relation case were better for wells 8, I1, and I6. This improvement would likely be more pronounced if less conductivity data were available.

The benefits of the seismic data were not fully achieved in this study because of computational limitations. Even with the fairly large cells used for the tracer simulations (1.5 m on a side and 0.45 m in the vertical direction), individual transport simulations took ~3 hours on a Hewlett Packard 755 workstation. The seismic data have a theoretical resolution of the order of 4–26 cm (calculated as the predominant wavelength of propagated seismic waves at the site divided by 4), which could provide more detailed information about the heterogeneities at this site than possible with the limited conductivity measurements. The actual resolution obtained from seismic tomography is probably on the 30–50 cm due to uncertainty in travel times, variable offset between wells and poor angular coverage across the imaged region.

5. Discussion and Conclusions

We have developed a new approach to integrate seismic and hydraulic information for aquifer property estimation. This approach involves estimating the relation between seismic slowness and aquifer properties of interest, such as lithology and hydraulic conductivity, using field scale measurements rather than using a lab-based relation. We can thus combine densely sampled cross-well tomographic slowness estimates with tracer and hydraulic information to estimate hydraulic conductivity fields. With this approach we not only determine the likely conductivity structure of an aquifer but we also explore the range of likely relations between slowness and conductivity at the field scale.

An a priori estimate of the relation between slowness and log conductivity can be developed from a number of data sources; however, field scale slowness estimates should be used when available. Laboratory slowness estimates are weakly correlated to the longer wavelength cross-well or surface seismic estimates due to factors such as frequency-dependent dispersion and sampling differences.

We demonstrate this approach using the Kesterson aquifer, California. We used cross-well seismic tomography in conjunction with hydraulic property estimates from cores and pump tests and a multiple-well tracer test to infer the relation between natural log hydraulic conductivity and seismic slowness for this alluvial aquifer. We found slowness to be positively correlated to hydraulic conductivity for this site. In this case, seismic slowness estimates provide high-resolution information about aquifer properties which is consistent with the local measurements of hydraulic conductivity.

For the Kesterson site, seismic travel times were used in conjunction with tracer concentration histories and a single drawdown measurement collected during the tracer test to provide three-dimensional slowness and hydraulic conductivity estimates. Simulation of two multiple-well tracer tests through the region provided reasonable matches to the measured concentration histories for five slowness realizations that were mapped into conductivity realizations using the estimated relations between slowness and log conductivity. The estimated relations were similar for these five slowness realizations because of the large number of slowness estimates between the injection and measurement locations.

Although the method worked well for the Kesterson site, it is currently limited by a variety of data requirements. The approach has been developed to take advantage of high-resolution crosswell tomography, which may be difficult to collect at many sites. This limits the application of the approach to aquifer sites where observation wells are available at

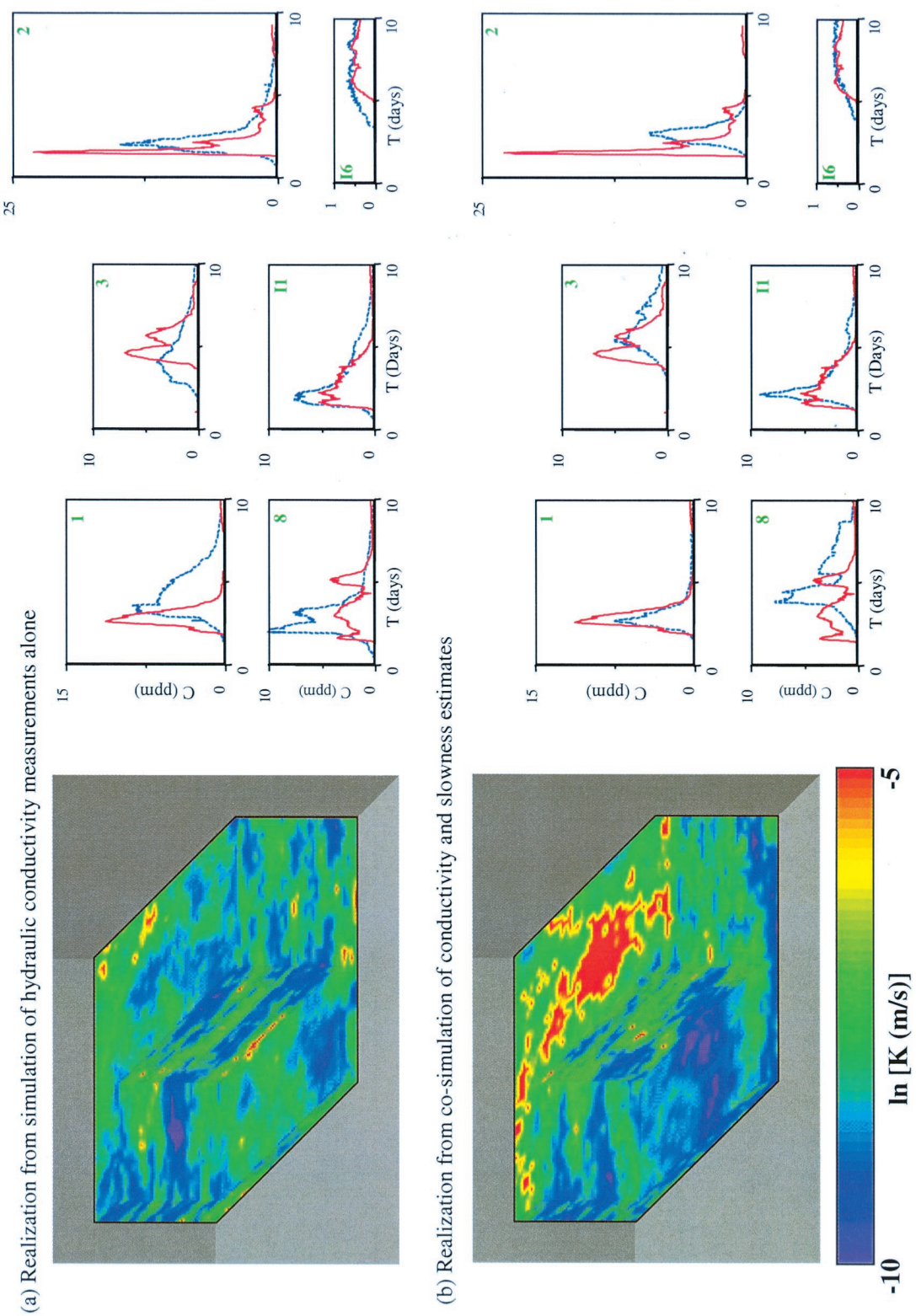

Plate 4. Comparison of tracer concentration histories for the 1986 fluorescein test simulated through conductivity realizations (a) generated using conductivity measurements alone and (b) generated using sequential Gaussian cosimulation with hard conductivity data and soft seismic slowness data from the fourth seismic realization.

a short enough spacing for cross-well geophysical imaging (<10 to 30 m depending on imaging method and aquifer materials). The method, as it is presented, requires tracer test data that may only be available at a limited number of contaminated sites.

In addition, different relations are expected for different depositional environments since lithology is the likely reason for changes in both slowness and hydraulic conductivity. In some cases, there may be no relation between slowness and hydraulic conductivity, while in others, a nonlinear or nonunique relation may exist. If a linear relation does not appear to describe the data, a more complex nonlinear relation may have to be estimated to extend the presented approach.

The data for combined geophysical and hydrologic inversions should be carefully collected to maximize their use. The well field needs to be carefully surveyed because small errors in the measured well locations can have a major impact on the estimated slowness values. For example, at the Kesterson site, well offsets had to be carefully corrected (<1%) to obtain consistent regional slowness estimates. The tracer test should be designed with as many wells as possible to provide sufficient sensitivity to the lateral and vertical variability in conductivity. Multilevel samplers with many vertical sampling locations would provide much more information about vertical variations in hydraulic conductivity within the aquifer. The hydraulic head should be measured at all possible locations during a tracer test to provide sensitivity to the mean conductivity value. Data collection involving tracer concentrations, drawdown measurements, and seismic travel times should be optimized to provide the maximum information about flow and transport properties.

The methods developed in this paper could likely be extended to incorporate a variety of other data types. For example, other attributes of the seismic data could be inverted to provide additional geophysical properties that may correlate to the hydraulic and lithologic properties of interest. For example, seismic attenuation may show significant correlation to hydraulic conductivity. The approach could perhaps also be used to infer the relation between the dielectric permittivity and hydraulic conductivity using ground-penetrating radar measurements.

Acknowledgments. We would like to thank Sally Benson, Ernie Majer, John Peterson, and Jill Geller of Lawrence Berkeley Laboratory for the Kesterson field data. We are also grateful for the financial support from National Science Foundation grants EAR-9316040 and EAR-9705812 and for the Hewlett Packard Company's grant of computer resources that made this project possible.

References

Benson, S. M., Characterization of the hydrogeologic and transport properties of the shallow aquifer under Kesterson reservoir, Ph.D. thesis, Univ. of Calif., Berkeley, 1988.

Benson, S. M., A. F. White, S. Halfman, S. Flexser, and M. Alavi, Groundwater contamination at the Kesterson reservoir, California, 1, Hydrogeologic setting and conservative tracer transport, *Water Resour. Res*., *27*(6), 1071–1084, 1991.

Beres, M. J., and F. P. Haeni, Application of ground-penetrating-radar methods in hydrogeologic studies, *Ground Water*, *29*(3), 375–386, 1991.

Bourbie, T., O. Coussy, and B. Zinszner, *Acoustics of Porous Media*, Gulf, Houston, Tex., 1987.

Copty, N., Stochastic characterization of subsurface flow parameters using geophysical and hydrological data, Ph.D. thesis, Univ. of Calif., Berkeley, 1994.

Copty, N., and Y. Rubin, A stochastic approach to the characterization of lithofacies from surface seismic and well data, *Water Resour. Res*., *31*(7), 1673–1686, 1995.

Copty, N., Y. Rubin, and G. Mavko, Geophysical-hydrological identification of field permeabilities through Bayesian updating, *Water Resour. Res*., *29*(8), 2813–2825, 1993.

Deutsch, C. V., and A. G. Journel, *Geostatistical Software Library and User's Guide*, Oxford Univ. Press, New York, 1992.

Han, D., A. Nur, and D. Morgan, Effect of porosity and clay content on wave velocity in sandstones, *Geophysics*, *51*, 2093–2107, 1986.

Hyndman, D. W., and S. M. Gorelick, Estimating lithologic and transport properties in three dimensions using seismic and tracer data: The Kesterson aquifer, *Water Resour. Res*., *32*(9), 2659–2670, 1996.

Hyndman, D. W., and J. M. Harris, Traveltime inversion for the geometry of aquifer lithologies, *Geophysics*, *61*(6), 1728–1737, 1996.

Hyndman, D. W., J. M. Harris, and S. M. Gorelick, Coupled seismic and tracer test inversion for aquifer property characterization, *Water Resour. Res*., *30*(7), 1965–1977, 1994.

Knoll, M. D., F. P. Haeni, and R. J. Knight, Characterization of a sand and gravel aquifer using ground-penetrating radar, Cape Cod, Massachusetts, *Water Resour. Invest. Tech. Rep*., *WRI 91-4034*, U.S. Geol. Surv., Washington, D. C., 1991.

Marion, D. P., A. Nur, H. Yin, and D. Han, Compressional velocity and porosity in sand-clay mixtures, *Geophysics*, *57*, 554–563, 1992.

McDonald, M. G., and A. W. Harbaugh, A modular three-dimensional finite-difference ground-water flow model, *Tech. Rep*., *TWRI 6-A1*, U.S. Geol. Surv., Washington, D. C., 1988.

McKenna, S. A., and E. P. Poeter, Field example of data fusion in site characterization, *Water Resour. Res*., *31*(12), 3229–3240, 1995.

Prasad, M., and R. Meissner, Attenuation mechanisms in sands: Laboratory versus theoretical (Biot) data, *Geophysics*, *57*(5), 710–719, 1992.

Raymer, D. S., E. R. Hunt, and J. S. Gardener, An improved sonic transit time-to-porosity transform, paper presented at the 21st Annual Meeting of the Society of Professional Well Log Analysts, Houston, Tex., 1980.

Rubin, Y., G. Mavko, and J. Harris, Mapping permeability in heterogeneous aquifers using hydrologic and seismic data, *Water Resour. Res*., *28*(7), 1809–1816, 1992.

Smart, P. L., and I. M. S. Laidlaw, An evaluation of some fluorescent dyes for water tracing, *Water Resour. Res*., *13*(1), 15–33, 1977.

Telford, W. M., L. P. Geldart, and R. E. Sheriff, *Applied Geophysics*, Cambridge Univ. Press, New York, 1990.

Wyllie, M. R., A. R. Gregory, and L. W. Gardner, Elastic wave velocities in heterogeneous and porous media, *Geophysics*, *21*, 41–70, 1956.

Zheng, C., MT3D: A modular three-dimensional transport model, S.S. Papadopulos and Assoc., Inc., Bethesda, Md., 1992.

S. M. Gorelick, Department of Geological and Environmental Sciences, Stanford University, Stanford, CA 94305.

J. M. Harris, Department of Geophysics, Stanford University, Stanford, CA 94305.

D. W. Hyndman, Department of Geological Sciences, Michigan State University, East Lansing, MI 48823.

(Received October 18, 1999; revised April 11, 2000;
accepted April 14, 2000.)